creative commons
COMMONS DEED

저작자표시-비영리-변경금지 2.0 대한민국

이용자는 아래의 조건을 따르는 경우에 한하여 자유롭게

- 이 저작물을 복제, 배포, 전송, 전시, 공연 및 방송할 수 있습니다.

다음과 같은 조건을 따라야 합니다:

저작자표시. 귀하는 원저작자를 표시하여야 합니다.

비영리. 귀하는 이 저작물을 영리 목적으로 이용할 수 없습니다.

변경금지. 귀하는 이 저작물을 개작, 변형 또는 가공할 수 없습니다.

- 귀하는, 이 저작물의 재이용이나 배포의 경우, 이 저작물에 적용된 이용허락조건을 명확하게 나타내어야 합니다.
- 저작권자로부터 별도의 허가를 받으면 이러한 조건들은 적용되지 않습니다.

저작권법에 따른 이용자의 권리는 위의 내용에 의하여 영향을 받지 않습니다.

이것은 이용허락규약(Legal Code)을 이해하기 쉽게 요약한 것입니다.

Disclaimer

dCollection

연세대학교
YONSEI UNIVERSITY

Evaluation of the Mechanical and Biological Properties of Polycaprolactone Scaffolds with Different Patterns Fabricated by the 3D Pen: A Novel *In Situ* Bone Repair Strategy

HongXin Cai

The Graduate School
Yonsei University
Department of Dental Science

연세대학교
YONSEI UNIVERSITY

Evaluation of the Mechanical and Biological Properties of Polycaprolactone Scaffolds with Different Patterns Fabricated by the 3D Pen: A Novel *In Situ* Bone Repair Strategy

A Dissertation Submitted
to the Department of Dental Science
and the Graduate School of Yonsei University
in partial fulfillment of the
requirements for the degree of
Doctor of Philosophy in Dental Science

HongXin Cai

December 2024

연세대학교
YONSEI UNIVERSITY

This certifies that the Dissertation of HongXin Cai is approved

Thesis Supervisor	Jae-Sung Kwon
Thesis Committee Member	Sung-Hwan Choi
Thesis Committee Member	Utkarsh Mangal
Thesis Committee Member	Sang-Bae Lee
Thesis Committee Member	Eun-Jung Lee

The Graduate School
Yonsei University
December 2024

연세대학교
YONSEI UNIVERSITY

ACKNOWLEDGEMENTS

I write this acknowledgment with immense excitement.

First and foremost, I would like to express my heartfelt gratitude to *Prof. Jae-Sung Kwon* for his unwavering support and guidance throughout my academic journey. From the very beginning of my studies to the completion of my Ph.D. degree, your encouragement has been instrumental in helping me grow, build confidence, and navigate my path forward. I am deeply thankful to *Prof. Sung-Hwan Choi*, *Prof. Utkarsh Mangal*, *Prof. Sang-Bae Lee*, and *Prof. Eun-Jung Lee* for their invaluable guidance on my dissertation. Your insightful feedback has profoundly enriched my work and significantly enhanced its quality. I also extend my sincere appreciation to *Prof. Kwang-Mahn Kim* and *Prof. Heng Bo Jiang* for their constructive suggestions and thoughtful input, which have greatly contributed to the depth and rigor of my research.

I want to acknowledge the incredible colleagues at the Department and Research Institute of Dental Biomaterials and Bioengineering. Your kindness made me feel at home here, enveloped in warmth and camaraderie. We have shared many wonderful memories that I will treasure. I also want to thank my friends who have accompanied me, it is your companionship and support that have allowed me to go firmly to today. In countless beautiful moments, we wrote this story together.

I owe a profound debt of gratitude to my family for their sacrifices; it is your unconditional love that has made me who I am today. Finally, I want to express my deepest thanks to my mother, *QingHua Tang*, for making all of this possible. She is great and deserving of the utmost respect. In places unseen, she has given so much silently. Thank you, Mom.

The snowy days at Yonsei, the sunsets over the Hangang River, and the illuminated N Seoul Tower under the night sky. These moments in South Korea over the past three years have been etched deeply into my memory. I will cherish them forever.

Thank you to all the people who have helped and inspired me along the way; you shine brightly in the river of my life. I love you all.

HongXin Cai

연세대학교
YONSEI UNIVERSITY

TABLE OF CONTENTS

연세대학교
YONSEI UNIVERSITY

연세대학교
YONSEI UNIVERSITY

LIST OF FIGURES

연세대학교
YONSEI UNIVERSITY

연세대학교
YONSEI UNIVERSITY

LIST OF TABLES

연세대학교
YONSEI UNIVERSITY

ABSTRACT

Evaluation of the Mechanical and Biological Properties of Polycaprolactone Scaffolds with Different Patterns Fabricated by the 3D Pen: A Novel *In Situ* Bone Repair Strategy

Interest and advancements in the field of bone tissue engineering (BTE) have grown significantly over the years, with a dramatic increase in the number of studies and reviews, since the mid-1980s. As one of the three elements of BTE, scaffolds have been widely studied and favored for their abilities to maintain the stability of bone defect sites for an extended period and to provide a favorable environment for the growth of osteoblasts and blood vessels.

To address the high cost and long cycle associated with the multi-step digital restoration process involving 3D printing technology, the 3D pen was proposed as an innovative strategy for *in situ* bone repair. *In situ* refers to processes occurring within a living organism or in its natural biological environment. Capitalizing on the low melting point characteristic of polycaprolactone (PCL), for the first time, the novel concept of directly constructing scaffolds at bone defect sites using 3D pens was introduced.

In this *in vitro* study, both the mechanical and biological properties of 3D pen-printed PCL scaffolds with six distinct patterns: unidirectional (UNI 0°, 45°, 90°); bidirectional (BID -45°/45°, 0°/90°); and concentric (CON), were meticulously evaluated. The bone repair scaffold creation process was simulated using a fused deposition modeling (FDM) 3D printer and a 3D pen by creating a cattle bone defect model to compare the achieved scaffold time efficiency and accuracy. Mechanical test results revealed that 3D pen-printed scaffolds with different patterns exhibited varying results in four tests, except the shear bond test. Optimal scaffold strength was consistently achieved when the printing direction was parallel to the applied force. Regarding biological properties, these scaffolds exhibited consistent cell viability over time and showcased excellent cell attachment capabilities overall. Furthermore, cells grew regularly along the printed filaments, with additional living cells at high elevations observed. Additionally, the 3D pen method outperformed traditional digital technology with an FDM 3D printer concerning accuracy and speed.

These findings underscored the tremendous potential of the 3D pen in the realm of medical science, specifically within the domain of *in situ* bone repair, characterized by its low cost, high speed, and convenience.

Key words : Bone tissue engineering, Scaffold, Polycaprolactone, 3D pen, *In situ* printing

연세대학교
YONSEI UNIVERSITY

1. INTRODUCTION

1.1. Bone tissue regeneration

The term regenerative medicine (RM) was first coined by Kaiser (Kaiser, 1992) in 1992, laying the tone for 21st-century medicine. However, the concept of tissue engineering (TE) can be traced back to 40 years ago; bone tissue engineering (BTE) began to garner attention around the mid-1980s and has since rapidly evolved (Amini et al., 2012; Langer and Vacanti, 1993).

Interest and advancements in the field of BTE have grown significantly over the years, with a dramatic increase in the number of studies and reviews published in the PubMed database since the mid-1980s. BTE aims to develop alternative treatment options that address the limitations of current clinical approaches, such as donor site morbidity, limited availability, immune rejection, and pathogen transfer. Achieving the ultimate goal of creating bone grafts that effectively enhance bone repair and regeneration requires the collaborative efforts of scientists, engineers, and surgeons (Amini et al., 2012).

BTE relies on a thorough understanding of bone structure, bone mechanics, and tissue formation to stimulate the development of new and functional bone tissues. Bones play an integral role in human life and health as one of the most crucial structures in the human body. In the dental field, atrophy of the upper and lower jaws caused by natural tooth loss or periodontal disease poses a significant problem (Zhao et al., 2021). Prompt and appropriate bone reconstruction to restore function is essential for both dentition repair and implant surgery. To date, the most commonly used method is bone graft granular material, also known as bone meal, which can be categorized into autogenous, allogeneic, xenogeneic, and alloplastic bone (Zhang et al., 2021). However, scholars have recently indicated that granular materials can easily collapse over time, leading to treatment failure due to insufficient stress support (Park et al., 2018). Additionally, granular material is unsuitable for large bone defects, such as leg bones, skulls, and pelvis (Dimitriou et al., 2011; Henkel et al., 2013; Staffa et al., 2012). Therefore, as one of the three elements of BTE, scaffolds have been widely studied and favored for their abilities to maintain the stability of bone defect sites for an extended period and to provide a favorable environment for the growth of osteoblasts and blood vessels (Bose et al., 2012; Hollister, 2005; Roseti et al., 2017).

연세대학교
YONSEI UNIVERSITY

1.2. Scaffold

Scaffolds are a crucial component of bone tissue engineering and are typically constructed from porous, degradable materials. These three-dimensional (3D) biocompatible structures are designed to replicate the extracellular matrix (ECM) properties, such as providing mechanical support, facilitating cellular activity, and promoting protein production through biochemical and mechanical interactions (Bose et al., 2012; Hollister, 2005). Scaffolds serve as templates for cell attachment and stimulate bone tissue formation *in vivo*. In addition to the material chemistry, critical parameters such as pore size, pore volume, and mechanical strength play a significant role in defining the performance of a scaffold. (Bose et al., 2012; Bose et al., 2013).

A successful scaffold must balance mechanical function with biofactor delivery, ensuring a smooth transition where the regenerated tissue gradually takes over the scaffold's function as it degrades (Hollister, 2005; Roseti et al., 2017). This often involves a trade-off between a denser scaffold, which offers better mechanical support, and a more porous scaffold, which enhances biofactor delivery. As the architect Robert le Ricolais once said, "The art of structure is where to put the holes." In the context of tissue engineering, a fitting paraphrase might be, "The art of scaffolding is where to place the holes and the biofactors" (Hollister, 2005).

In dentistry, patients undergoing dental surgery may experience loss of teeth accompanied by extensive alveolar bone defects resulting from tumors, trauma, or severe periodontal diseases (Park et al., 2018; Wang et al., 2022). To address both the biological and functional loss in the oral cavity, comprehensive reconstruction procedures are frequently carried out, often involving the implantation of multiple dental implants. 3D porous scaffolds play a crucial role in these procedures by maintaining the physical space needed for bone regeneration. They help prevent the invasion of unwanted cells, anchor endogenous osteogenic cells to promote cell ingrowth and provide a conducive molecular environment for osteoblastic differentiation (Park et al., 2018).

연세대학교
YONSEI UNIVERSITY

1.3. Computer-aided design and computer-aided manufacturing (CAD/CAM)

Porous bone scaffolds can be fabricated using a wide range of materials and methods, including chemical/gas foaming, solvent casting, particle/salt leaching, freeze drying, thermally induced phase separation, and foam-gel techniques. While these methods are widely used, they offer limited control over key factors such as pore size, shape, and interconnectivity. Additionally, creating scaffolds with customized porosity to suit specific defects remains challenging with most of these techniques (Bose et al., 2013).

With the continuous innovation of digital technology, 3D printing has become an increasingly mature technique for scaffold fabrication (Bose et al., 2013; Roseti et al., 2017). The process involves obtaining a digital file of the patient's bone defect using either cone beam computed tomography (CBCT) or dental scanners, importing it into computer-aided design (CAD) software for restoration design, and printing the designed model, which can be tried on or implanted (Rekow, 2020). Fused deposition modeling (FDM)-type 3D printers are commonly used for fabricating polymer scaffolds using thermoplastic filaments (Wickramasinghe et al., 2020). In slicing software, the porosity and pattern of the scaffold can be precisely controlled. The adjustable nozzle temperature allows for the use of various materials, such as polycaprolactone (PCL), poly (lactic-co-glycolic acid) (PLGA), polylactic acid (PLA), and even composite filaments.

However, although the CAD/CAM method can provide effective tissue repair and functional recovery, it raises the treatment threshold, increases medical costs, imposes high requirements on equipment and software, and may not be sufficient in emergencies, such as bone fractures and trauma caused by accidents, where immediate repair is urgently needed (Dimitriou et al., 2011). Therefore, there is a need to explore an increasingly efficient method.

연세대학교
YONSEI UNIVERSITY

1.4. *In situ* bioprinting and 3D pen

"*In situ*" is a Latin term meaning "in its original place" or "in position." In medicine and science, it refers to processes occurring within a living organism or in its natural biological environment. *In situ* bioprinting—also known as *in vivo* bioprinting—involves the direct deposition of bioinks to create or repair living tissues or organs directly at the defect site in a clinical setting (Singh et al., 2020). This concept was first introduced by Campbell in 2007 (Campbell and Weiss, 2007). The target site for *in situ* bioprinting is typically an anatomical location in the body requiring regeneration, like skin, cartilage, and bone (Chaudhry and Czekanski, 2023; Xie et al., 2022).

The *in situ* tissue engineering (TE) approach offers significant advantages by eliminating the need to create an artificial microenvironment, which is critical for tissue development (MacAdam et al., 2022). In contrast, *ex vivo* methods often require replicating the native tissue microenvironment, including essential biochemical and biophysical cues, to support cell viability, proliferation, differentiation, and migration—processes essential for the formation of functional tissues or organs (Singh et al., 2020). The natural presence of these factors in *in situ* approaches, along with their simplicity, ease of application, reduced costs, lower labor demands, and potentially fewer regulatory hurdles, makes *in situ* strategies a more appealing option for TE applications compared to *ex vivo* methods (Mahmoudi et al., 2023).

The 3D pen is a handheld 3D printing tool that allows users to draw and create 3D objects by extruding heated plastic filaments (Ligon et al., 2017). As a compact and affordable alternative to traditional 3D printers, 3D pen offers additional flexibility and freedom without the need for a computer or software (de Oliveira et al., 2020). Therefore, 3D pen is being considered as a novel *in situ* bioprinting technology. Studies by Arora and Bhati (Arora and Bhati, 2020) have shown that 3D pen-printed polylactic acid (PLA) scaffolds have superior mechanical properties to scaffolds printed by a fused deposition modeling (FDM) printer. de Araujo et al. (de Araujo et al., 2020) confirmed that 3D pen-printed composite filaments made of polycaprolactone (PCL)/nanohydroxyapatite (nHap)/laponite (Lap) are nontoxic and can promote the proliferation of fibroblasts. Consequently, the use of a 3D pen to print biological scaffolds directly into patient's bone defects was proposed as a highly efficient and customizable approach for bone repair (Fig. 1). As a Food and Drug Administration (FDA)-approved degradable biomaterial, PCL is safe and exhibits good biocompatibility and mechanical properties (Puppi et al., 2010; Stevens, 2008). Numerous scholars have demonstrated that PCL is an ideal base material and coating for bone repair scaffolds, and its microsphere structure can promote the integration of new blood vessels (Pierantozzi et al., 2020; Roohani-Esfahani et al., 2010; Salerno et al., 2022; Shahverdi et al., 2022; Shen et al., 2019; Wang et al., 2022). PCL can be combined with other biomaterials, such as hydroxyapatite and calcium carbonate, to enhance its performance in guiding bone tissue regeneration. This combination resulted

연세대학교
YONSEI UNIVERSITY

in excellent bioactivity and support for tissue healing and growth (Beatrice et al., 2020a; Ngo et al., 2023; Park et al., 2018). Moreover, the low melting point of PCL, which ranges from 59 to 64 ℃, is a significant advantage, allowing it to reach a fluid state at approximately 50 ℃ (Sinha et al., 2004; Woodruff and Hutmacher, 2010). This property makes it an excellent choice for 3D pens on bone repair scaffolds. Given that the printing direction and pattern significantly influence scaffold performance (Mishra et al., 2021; Zaldivar et al., 2017), it is essential to investigate the effects of 3D pen printing patterns on scaffold properties.

연세대학교
YONSEI UNIVERSITY

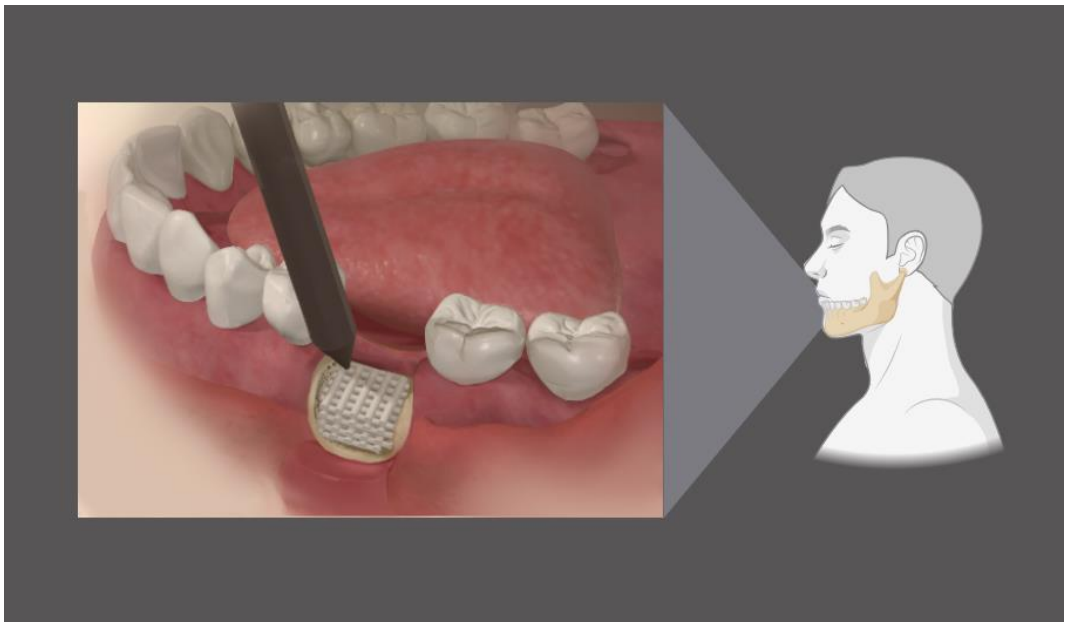

<Fig 1> Process of printing PCL scaffolds at bone defect sites using a 3D pen.

연세대학교
YONSEI UNIVERSITY

1.5. Research objective and null hypothesis

In this *in vitro* study, the mechanical and biological properties of 3D pen-printed scaffolds with different patterns are evaluated. Scaffolds printed by an FDM printer are used for reference. Additionally, the process of creating a repair scaffold is simulated using traditional digital technology and a 3D pen by making a bone defect model, comparing the time required and accuracy of the achieved scaffolds. The null hypothesis is that there are no significant differences in the mechanical and biological properties of PCL scaffolds with different patterns produced by 3D pen and scaffolds produced by FDM 3D printer.

연세대학교
YONSEI UNIVERSITY

2. MATERIALS AND METHODS

2.1. Sample preparation

2.1.1. Reference group

Poly(ε-caprolactone) 3D printer filaments (Φ1.75 mm, SUNLU, Guangdong, China) were used in the experiments. AutoCAD 2022 (AUTODESK, San Francisco, CA, USA) was chosen to design the required model, and the model standard tessellation language (STL) format file was generated and imported into the slicing software program (Cubicreator4 V4.4.0, CUBICON, Seongnam-si, Korea). After configuring the optimal performance parameters, the file was transferred to the FDM 3D printer (Single Plus, CUBICON, Seongnam-si, Korea) in G-code format to obtain the scaffolds. (Specific parameters: 0.2 mm layer height, 100 % infill density, 70 ℃ default printing temperature, 50 ℃ build plate temperature, 100 % flow, and 60 mm/s print speed)

2.1.2. Experimental group

The same PCL filament and 3D pen (SUNLU, Guangdong, China) with a product length of 175 mm and a nozzle diameter of 0.7 mm were used. The experimental group was divided into three categories and six groups according to different printing directions: unidirectional (UNI 0°, 45°, 90°); bidirectional (BID -45°/45°, 0°/90°); concentric (CON) (Fig. 2). The scaffolds were printed along pre-drawn routes to ensure precise overall dimensions at 70 ℃. The 3D pen was operated by a single experienced and extensively trained individual. During the experiments, the contours of different desired samples on the desktop were outlined in advance, and the models were manually built on this foundation (Fig. 3). The extruded polymer solidified in about ten seconds.

연세대학교
YONSEI UNIVERSITY

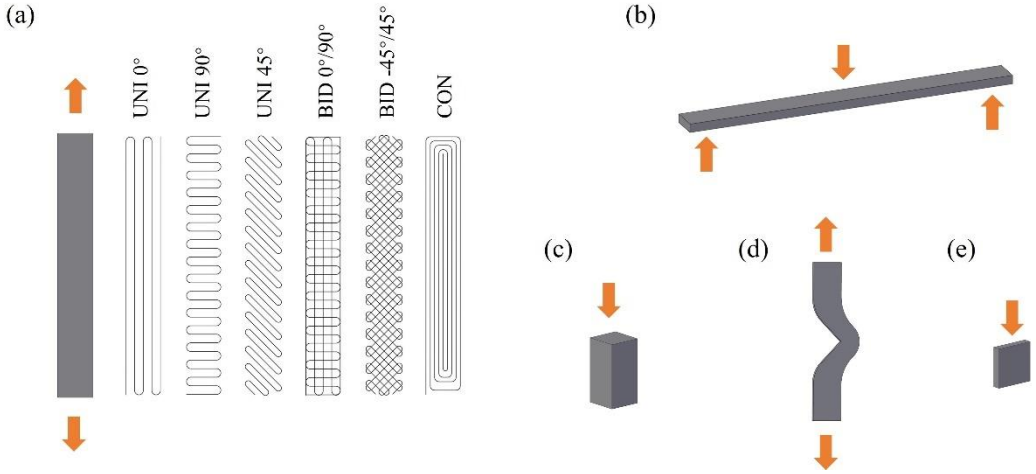

<Fig 2> Three-dimensional specimen designs for various mechanical property tests. (a) Classification of experimental groups using tensile specimens as an example: unidirectional (UNI 0°, 45, 90); bidirectional (BID 0°/90°, -45°/45°); and concentric (CON). Here, 0° refers to the direction parallel to the applied force, with the long axis of the flexural specimen also aligned at 0°. (b) Flexural test specimen. (c) Compressive test specimen. (d) Tear test specimen. (e) Shear bond test specimen. Orange arrows indicate the direction of the applied force.

연세대학교
YONSEI UNIVERSITY

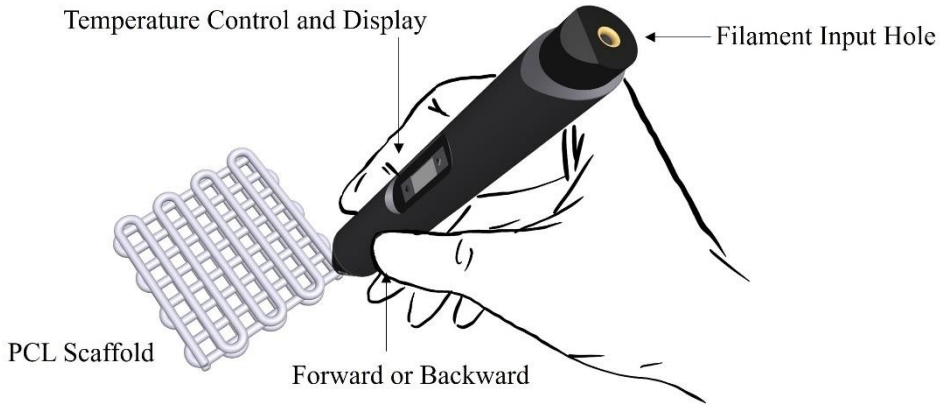

<Fig 3> Experimental group operation illustration with function introduction of a 3D Pen.

연세대학교
YONSEI UNIVERSITY

2.2. Evaluation of mechanical properties

The evaluation of the mechanical properties was performed by a computer-controlled universal testing machine (5942, INSTRON, Norwood, MA, USA). To maximize the number of printed lines and layers in each sample, while emphasizing the impact of different printing directions, the model specifications were based on standardized guidelines that utilized larger-scale models. This approach allowed for a more comprehensive analysis of mechanical behavior, taking into account the structural variations introduced by the different printing orientations.

연세대학교
YONSEI UNIVERSITY

2.2.1. Tensile test

In reference to American Society for Testing Materials (ASTM) D 3039, the dimensions of the tensile test specimens were set to 150 mm × 20 mm × 2 mm with tab lengths of 25 mm at both ends (Fig. 2a). Six specimens in each group were forced by the crosshead at 5.0 mm/min until failure. For the groups without significant fracture, the machine continued to apply force until the maximum tensile strength of the specimen was exceeded. The maximum force and maximum extension were recorded, the maximum tensile stress and modulus of elasticity were calculated according to the formulas provided in the standard (below), and the stress-strain curves were plotted. Scanning electron microscopy (SEM) (JSM-IT500HR, JEOL, Tokyo, Japan) was used to examine the specimens printed using the FDM 3D printer.

(1) $\sigma = P/A$

(2) $\varepsilon = \delta/L_g$

(3) $E = \Delta\sigma/\Delta\varepsilon$

where σ is the tensile stress, expressed in MPa; P is the load, expressed in N; A is the cross-sectional area, expressed in mm^2; ε is the tensile strain; δ is the extensometer displacement, expressed in mm; L_g is the extensometer gage length, expressed in mm; and E is the modulus of elasticity, expressed in MPa.

2.2.2. Flexural test

For the flexural test, specimens were fabricated following ASTM D 7264 standards, with precise dimensions of 154 mm × 13 mm × 4 mm and a support span of 128 mm (Fig. 2b). The test was conducted at a crosshead movement speed of 5.0 mm/min and the machine automatically terminated the test after 6 minutes. Following the completion of the test, the flexural stress and modulus were calculated based on the recorded data. The corresponding curves were then plotted, following the same approach as used in the tensile test experiments.

연세대학교
YONSEI UNIVERSITY

2.2.3. Compressive test

In accordance with ASTM D695-02a standard, the prism samples were prepared at 10 mm × 10 mm × 20 mm (Fig. 2c). The crosshead applied a continuous compression at a rate of 1.3 mm/min until a maximum force of 1 kN was reached. Throughout the test, data were meticulously recorded, and the compressive modulus for each group of samples was subsequently calculated based on the collected data.

2.2.4. Tear test

The shape and size of the tear sample were consistent with ASTM D1004-21 standard (Fig. 2d). During testing, the grip moved at a constant speed of 51 mm/min until the specimen fractured. The mean maximum resistance to tearing was calculated for each group of six samples, and the representative load–extension curves were plotted to visualize the tearing behavior across different groups.

2.2.5. Shear bond strength

Fig. 4 depicts the test method for measuring the shear bond strength between 3D pen-printed PCL samples and bone. A cattle bone block was securely fixed into the test clamp, and a 10 mm × 10 mm × 2 mm PCL specimen was printed on the bone surface using a 3D pen (Fig. 2e). After 1 or 5 minutes, the shear blade moved downwards at a speed of 1 mm/min until the sample was delaminated. The bond strength was calculated according to the formula provided in the international standard ISO 29022 (2018):

$\sigma = F/A_b$

where σ is the stress, expressed in MPa; F is the force, expressed in N; and Ab is the bonding area, expressed in mm^2.

연세대학교
YONSEI UNIVERSITY

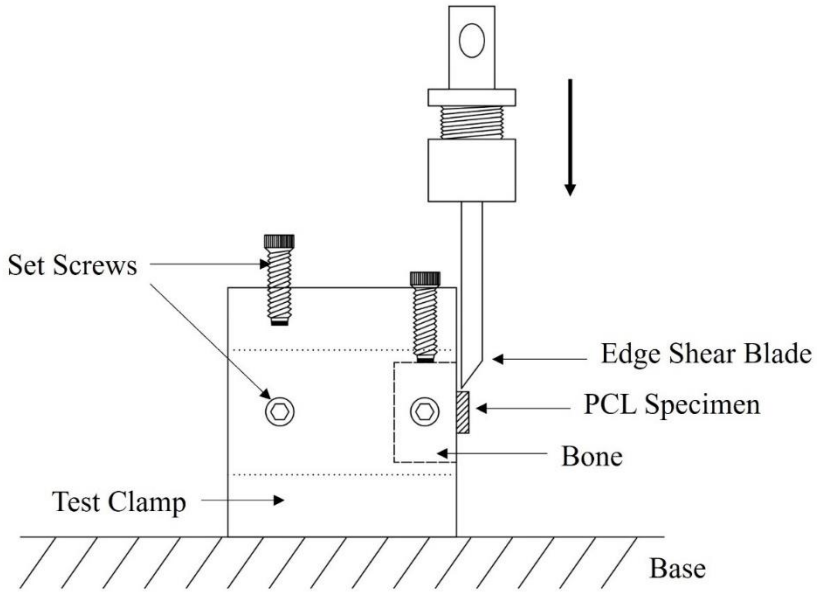

<Fig 4> Schematic diagram of testing the shear bond strengths of 3D pen-printed PCL samples to the cattle femur bone.

연세대학교
YONSEI UNIVERSITY

2.3. Evaluation of biological properties

The murine pre-osteoblast cell line MC3T3-E1 (Lonza, Basel, Switzerland) was selected to evaluate the biological performance of the scaffolds. Since the experimental samples, which were cylindrical in shape with a diameter of 10 mm and a height of 2 mm, were created using the 3D pen, this group was further divided into three groups: UNI, BID, and CON. Prior to testing, all samples were soaked in absolute ethanol for 1 hour, followed by sterilization under ultraviolet light for 24 hours to ensure a sterile environment for subsequent cell culture experiments.

연세대학교
YONSEI UNIVERSITY

2.3.1. Cell viability

The EZ-Cytox Enhanced Cell Viability Assay Kit (DoGenBio, Seoul, Korea) was used to detect the proportion of living cells. A total of 1.5×10^5 cells per well were seeded in 48-well plates with scaffolds containing 400 μL of minimum essential medium α (α-MEM, WEL GENE, Gyeongsan-si, Korea) supplemented with 10 % of foetal bovine serum, 1 % of antibiotics, 200 μM of ascorbic acid, and 10 mM of β-glycerophosphate. The same volume of cell suspension was placed into the blank well as the control group, while the blank group contained only α-MEM. After culturing 1, 4, and 7 days in an incubator with 5 % CO_2, 37 ℃, and > 90 % humidity, the culture medium was carefully removed and rinsed twice with phosphate-buffered saline (PBS) (WELGENE, Gyeongsan-si, Korea). Then, 400 μL of medium and 40 μL of WST-1 reagent were added to each well. Before transferring to a new plate and detecting the absorbance at 450 nm by a microplate reader (Epoch, BioTek, Incheon, Korea), the well plate was placed on an incubated shaker (Lab Companion, Daejeon, Korea) for 1 miniute to ensure that the system to be tested was fully mixed. Cell viability was calculated by the following formula:

Cell Viability (%) = (Exp. – Blank) / (Control – Blank) × 100 %

A LIVE/DEAD Viability/Cytotoxicity Kit (Invitrogen, Thermo Fisher Scientific, MA, USA) was utilized for cellular staining. In 24-well plates, 2.5×10^5 cells per well were seeded onto scaffolds. After the cells were cultured for 24 hours in an incubator with 5 % CO_2, 37 ℃, and > 90 % humidity, the medium was gently removed, and the scaffolds were fully washed with PBS to eliminate residual esterase activity. A sufficient staining solution, containing 2 μM of Calcein AM and 4 μM of EthD-I, was added to each well. The cells were then observed through confocal laser scanning microscopy (CLSM) (LSM 900 with Airyscan 2, ZEISS, Jena, DE) after 20 minutes of culture in the dark.

연세대학교
YONSEI UNIVERSITY

2.3.2. Cell attachment

To assess cell attachment, 2.5×10^5 cells per well were seeded onto scaffolds and incubated for 24 to 72 hours. The cells were fixed with 4 % paraformaldehyde (PFA) (Wako, FUJIFILM, Tokyo, Japan) for 30 minutes and rinsed twice with PBS. The scaffolds were split into two batches for further analysis. One batch was dehydrated through ethanol gradients from 50 % to absolute ethanol and allowed to dry naturally overnight. The morphologies of cells were examined using scanning electron microscopy (SEM) (JSM-IT500HR, JEOL, Tokyo, Japan). In the other batch, the cells were permeabilized using 0.1 % Triton X-100 (Sigma, Merck, Darmstadt, Germany) in phosphate buffer for 10 minutes, stained with 100 nM of rhodamine-phalloidin (TRITC Phalloidin, Thermo Fisher Scientific, MA, USA) for 40 minutes, and then observed and photographed using CLSM.

연세대학교
YONSEI UNIVERSITY

2.4. Simulated *in vitro* test

Through the simulated *in vitro* test, the fabrication speed and the accuracy values of scaffolds were compared between the traditional digital process with an FDM 3D printer and a novel method involving a 3D pen. A portion of the cattle femur was extracted to make a bone defect model of 30 mm × 10 mm × 5 mm. In the traditional group, the digital file of the bone model was obtained by an extraoral scanner (MEDIT, Seoul, Korea) and imported into the modeling software (Geomagic Freeform Plus, 3D SYSTEMS, South Carolina, USA) for scaffold design. The STL format file of the generated scaffold was imported into the FDM 3D printer to obtain the physical scaffold (Fig. 5). The above steps were repeated six times, and the duration was recorded. In the novel method group, repair scaffolds were directly printed in the bone defect by an experienced person with a 3D pen for all six patterns. The length, width, and height of each scaffold were measured with a caliper, and the volume was calculated. The actual dimensions of the bone defect model were measured using a micrometer (Mitutoyo, Kawasaki, Japan) as the gold standard.

연세대학교
YONSEI UNIVERSITY

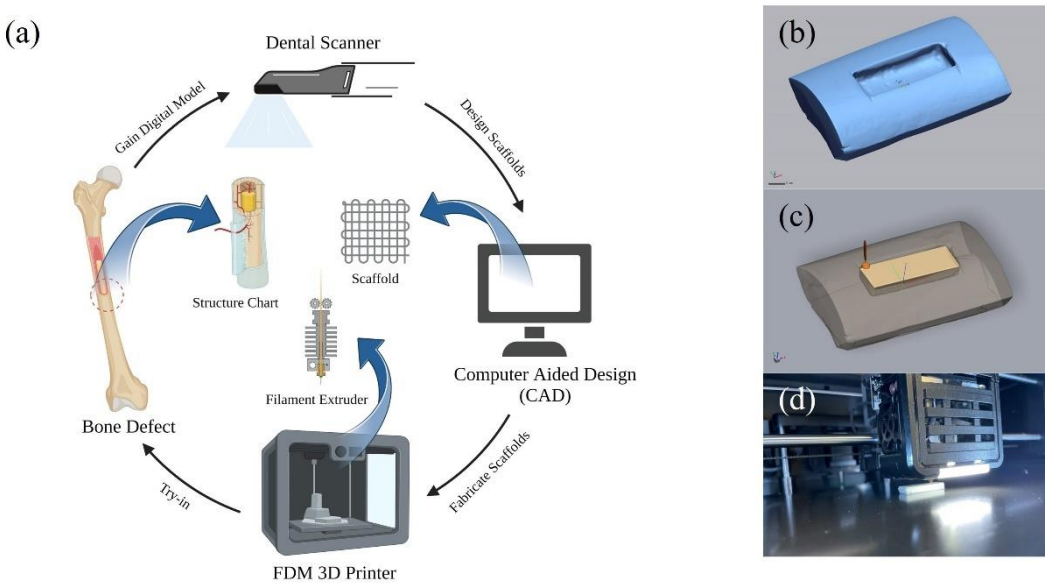

<Fig 5> Traditional group of simulated *in vitro* tests. (a) Procedures of digitally assisted treatment of bone defects, including scanning, CAD, and CAM (created with BioRender.com). (b) The 3D file of cattle bone with a square bone defect by scanning. (c) Bone repair scaffold design through industrial modeling software. (d) Fabrication of the scaffold by an FDM 3D printer.

연세대학교
YONSEI UNIVERSITY

2.5. Statistical analysis

Statistical analysis was performed using commercially available software (International Business Machines (IBM) Statistical Product and Service Solutions (SPSS) Statistics 26.0) by one-way analysis of variance (ANOVA). All data were expressed as the mean ± standard deviation. Differences between groups were analyzed using Tukey's post hoc test. A t-test was applied to each group in the shear bond strength test. A p-value of < 0.05 was considered statistically significant.

연세대학교
YONSEI UNIVERSITY

3. RESULTS

3.1. Tensile test results

Figs. 6 and 7 present the results of the tensile test. The groups containing filament print directions of 0° (parallel to the tension) all exhibited high ductility, while the other groups fractured within 8 % strain (Fig. 6a). Among the tested groups, the CON group demonstrated the greatest tensile strength, the UNI 90° group displayed the smallest tensile strength, and there was no significant difference between the two groups printed bidirectionally. The results of the elastic modulus closely mirrored those of the maximum tensile stress; statistically, the FDM group was the lowest. Notably, the tensile strength of the BID 0°/90° group was significantly higher than that of the UNI 90° group (Fig. 6b). Clear observations from photographs revealed that the filaments printed at 0° were all stretched to very long lengths, and the 45° and 90° filaments and the FDM group had no traces of elongation (Fig. 7). The filaments produced by the FDM 3D printer were fine due to the nozzle diameter. Besides, despite setting the fill density to 100 %, tiny pores were still present in the printed specimen, instead of the solid structure typically expected. Through the SEM image, the pores can be observed in the FDM group samples, with the spacing between the printed filament groups (two filaments per group) being approximately 100 μm (Fig. 7a). Compared to 3D printed filaments, the filaments of the specimen produced by 3D pen were about twice as large, about 500 microns (Fig. 7b).

연세대학교
YONSEI UNIVERSITY

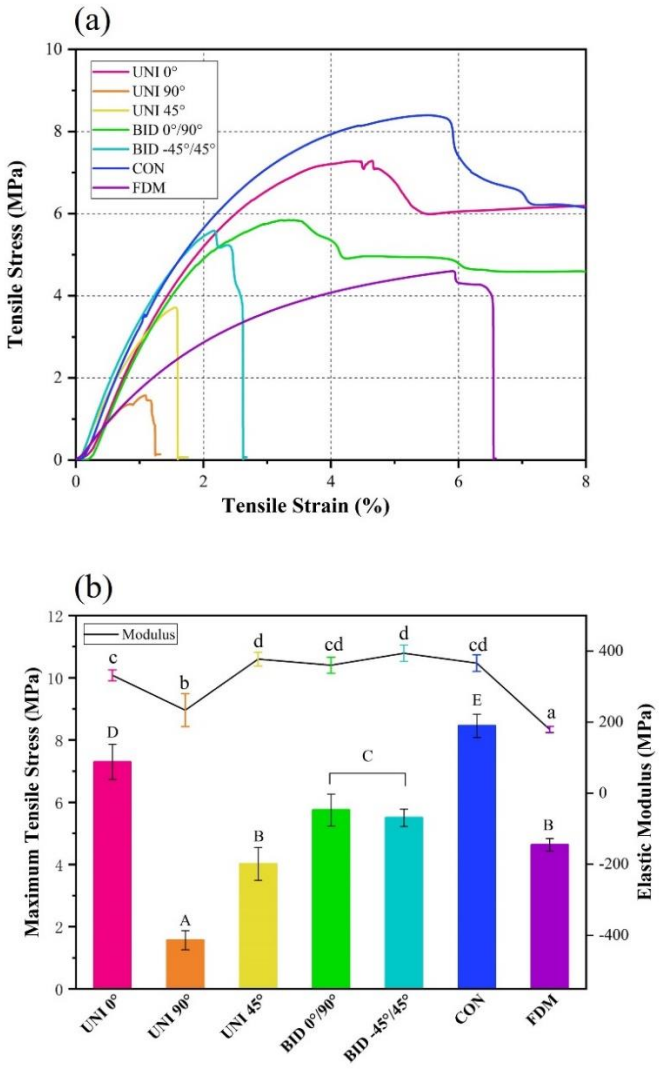

<Fig 6> (a) Representative stress-strain curves for seven groups of the tensile test. (b) Maximum tensile stress (bar graph) and tensile modulus of elasticity (line graph) values of the specimens. Differences in uppercase and lowercase alphabetical letters indicate significant differences between the groups ($n = 6$, $p < 0.05$).

연세대학교
YONSEI UNIVERSITY

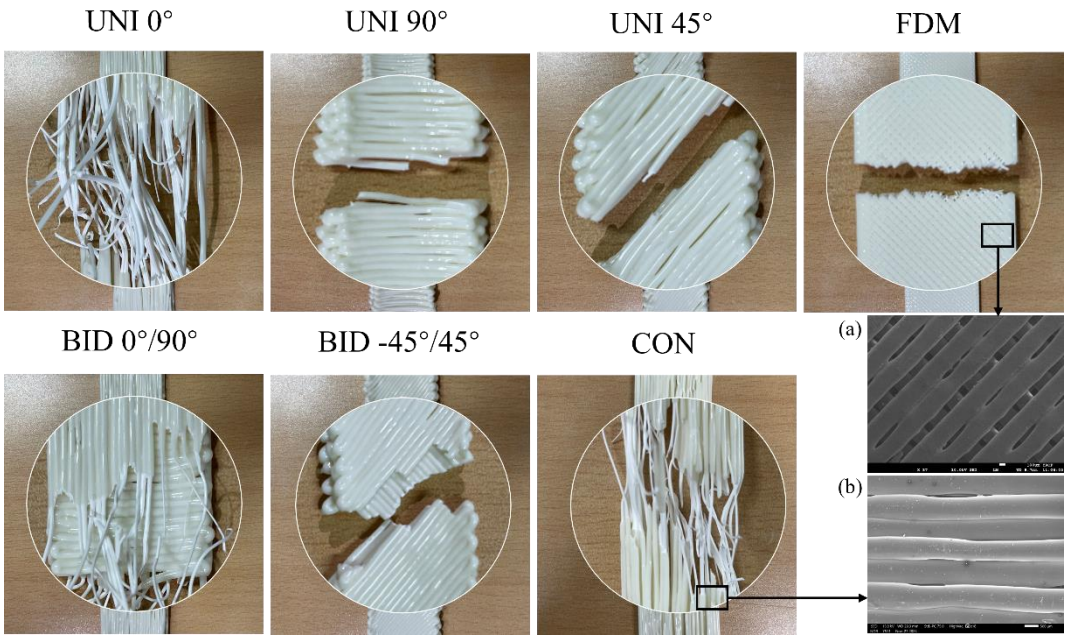

<Fig 7> Digital photographs of tensile specimen failure parts, and SEM images of printed filaments in FDM group (a) and 3D pen group (b).

연세대학교
YONSEI UNIVERSITY

3.2. Flexural test results

Fig. 8 presents the results of a flexural test conducted in this study. At the outset, all groups exhibited a comparable trend until the flexural strength reached 3 MPa (Fig. 8a). Beyond this range, the UNI 90° and BID 0°/90° groups fractured successively, likely attributed to the existence of the 90° filaments. Following these fractures, the curves of the remaining groups displayed noticeable fluctuations, except for the UNI 0° group, and the UNI 45° group was the most obvious.

연세대학교
YONSEI UNIVERSITY

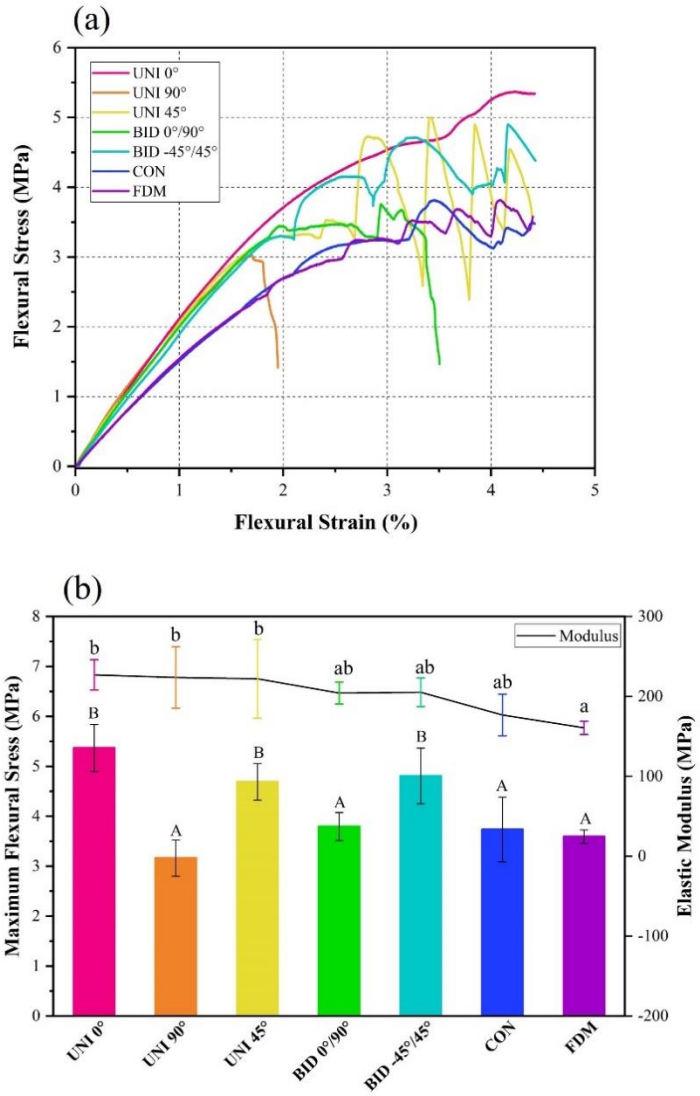

<Fig 8> (a) Representative stress−strain curves for seven groups of the flexural test. (b) Maximum flexural stress (bar graph) and flexural modulus of elasticity (line graph) values of the specimens (n = 6, $p < 0.05$).

연세대학교
YONSEI UNIVERSITY

3.3. Compressive test results

During the compression test, the PCL specimens exhibited no signs of fracture. As a result, the comparison was focused only on the compressive modulus of each sample group under the maximum load capacity (Fig. 9). Samples that were printed with filaments either parallel or perpendicular to the pressure performed well.

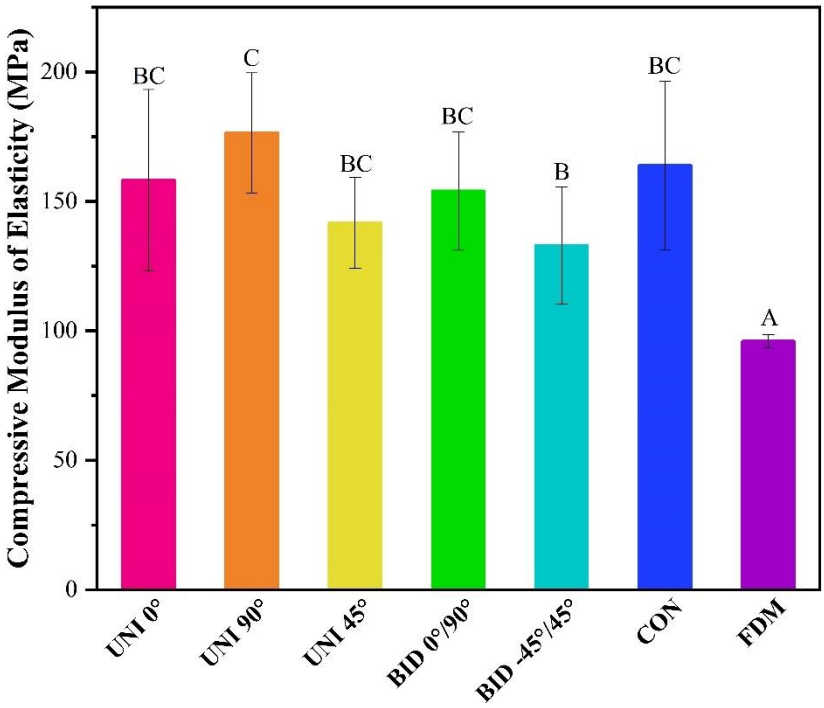

<Fig 9> Modulus of elasticity values for seven groups of the compressive test (n = 6, $p < 0.05$).

연세대학교
YONSEI UNIVERSITY

3.4. Tear test results

Group UNI 0° had the greatest resistance to tearing, followed by group BID 0°/90° and CON (Fig. 10). As with the tensile test results, the resistance to tearing of the BID 0°/90° group was significantly higher than that of the UNI 90° group. The best tear strength of the scaffold could be achieved by printing in a direction parallel to the tearing force using the 3D pen. Additionally, the tear strength of the bidirectional 45°-printed sample was significantly better than that of the unidirectional-printed sample (Fig. 10b).

연세대학교
YONSEI UNIVERSITY

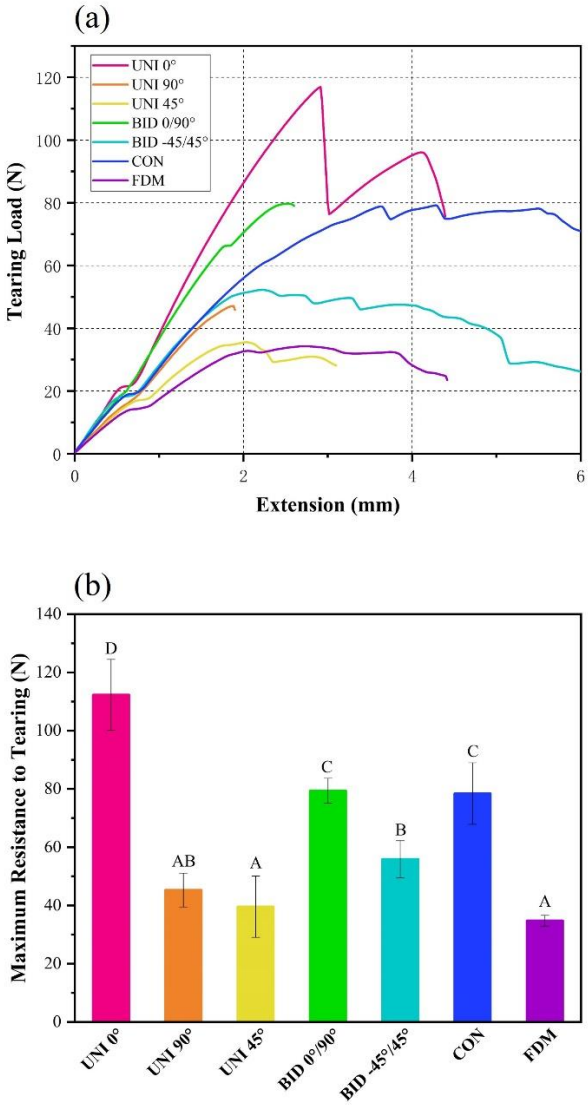

<Fig 10> (a) Representative load−extension curves for seven groups of the tear test. (b) Maximum resistance to tearing of the specimens (n = 6, $p < 0.05$).

연세대학교
YONSEI UNIVERSITY

3.5. Shear bond test results

Fig. 11 presents the bond strength results of 3D pen-printed PCL specimens and cattle bone. Statistical analysis indicated that there was no significant difference in the bond strength of each group at either 1 or 5 minutes. Over time, the strengths of all groups significantly decreased except for BID -45°/45°, reaching approximately 20×10^{-3} MPa after 5 minutes (Table 1).

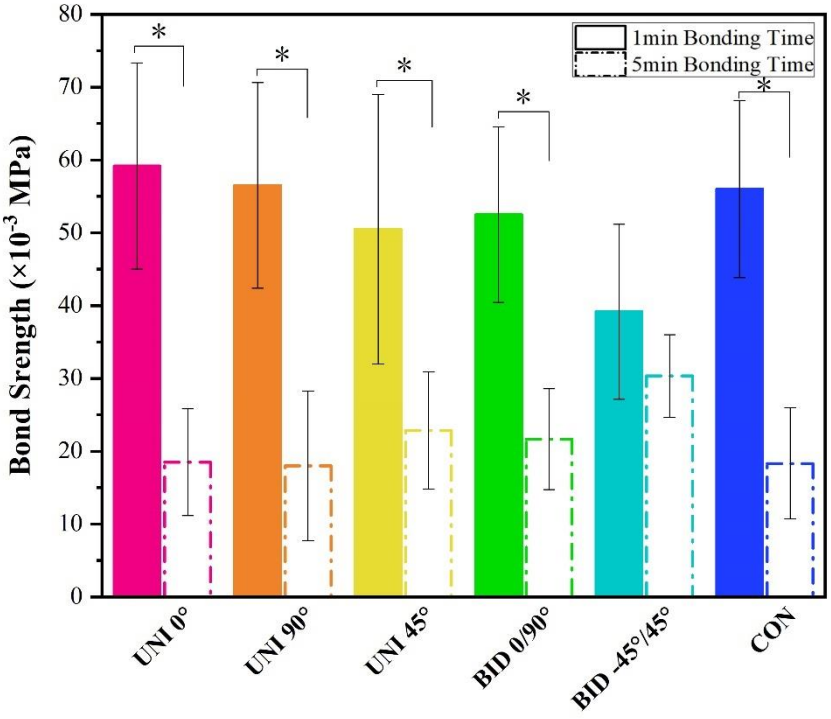

<Fig 11> Bond strengths of 3D pen-printed specimens to cattle bone after 1 min ($n = 6$, $p > 0.05$) and 5 min ($n = 6$, $p > 0.05$). In the inter-group comparison, there were significant differences except for BID -45°/45° ($p < 0.05$).

연세대학교
YONSEI UNIVERSITY

Table 1. Experimental results of mechanical properties testing (mean ± standard deviation, with two decimal places retained). Uppercase letters indicate statistically significant differences between different groups, while lowercase letters denote statistical differences within groups for bond strength comparison ($p < 0.05$). A: Maximum Tensile Stress (MPa); B: Tensile Modulus of Elasticity (MPa); C: Maximum Flexural Stress (MPa); D: Flexural Modulus of Elasticity (MPa); E: Compressive Modulus of Elasticity (MPa); F: Maximum Resistance to Tearing (N); G: 1 min Bond Strength ($\times 10^{-3}$ MPa); H: 5 min Bond Strength ($\times 10^{-3}$ MPa).

	UNI 0°	**UNI 90°**	**UNI 45°**	**BID 0°/90°**	**BID -45°/45°**	**CON**	**FDM**
A	7.30 ± 0.56^{D}	1.57 ± 0.31^{A}	4.02 ± 0.53^{B}	5.75 ± 0.51^{C}	5.50 ± 0.28^{C}	8.46 ± 0.37^{E}	4.63 ± 0.20^{B}
B	331.73 ± 15.40^{C}	233.79 ± 46.40^{B}	377.42 ± 19.18^{D}	360.18 ± 22.53^{CD}	393.92 ± 22.98^{D}	366.13 ± 23.50^{CD}	179.41 ± 8.84^{A}
C	5.37 ± 0.47^{B}	3.16 ± 0.36^{A}	4.69 ± 0.36^{B}	3.80 ± 0.28^{A}	4.81 ± 0.56^{B}	3.74 ± 0.65^{A}	3.59 ± 0.13^{A}
D	227.00 ± 18.90^{B}	223.78 ± 38.53^{B}	222.12 ± 49.37^{B}	204.30 ± 13.73^{AB}	205.23 ± 17.93^{AB}	176.81 ± 26.02^{AB}	160.81 ± 8.40^{A}
E	158.17 ± 35.06^{BC}	176.50 ± 23.18^{C}	141.67 ± 17.55^{BC}	154.00 ± 22.85^{BC}	133.00 ± 22.53^{B}	163.83 ± 32.70^{BC}	95.97 ± 2.63^{A}
F	112.33 ± 12.16^{D}	45.31 ± 5.82^{AB}	39.60 ± 10.52^{A}	79.40 ± 4.25^{C}	55.90 ± 6.35^{B}	78.45 ± 10.57^{C}	34.78 ± 1.84^{A}
G	59.17 ± 14.16^{b}	56.50 ± 14.11^{b}	50.50 ± 18.50^{b}	52.50 ± 12.08^{b}	39.17 ± 12.01	56.00 ± 12.19^{b}	N/A
H	18.50 ± 7.34^{a}	18.00 ± 10.26^{a}	22.83 ± 8.06^{a}	21.67 ± 6.92^{a}	30.33 ± 5.68	18.33 ± 7.63^{a}	N/A

연세대학교
YONSEI UNIVERSITY

3.6. Cell viability results

3.6.1. Quantitative analysis

Quantitative analysis revealed that the cell viability was significantly highest in the UNI group on day 1 (Fig. 12). However, by the fourth and seventh days, there was no difference among the three 3D pen groups, while the FDM group consistently exhibited the lowest cell viability.

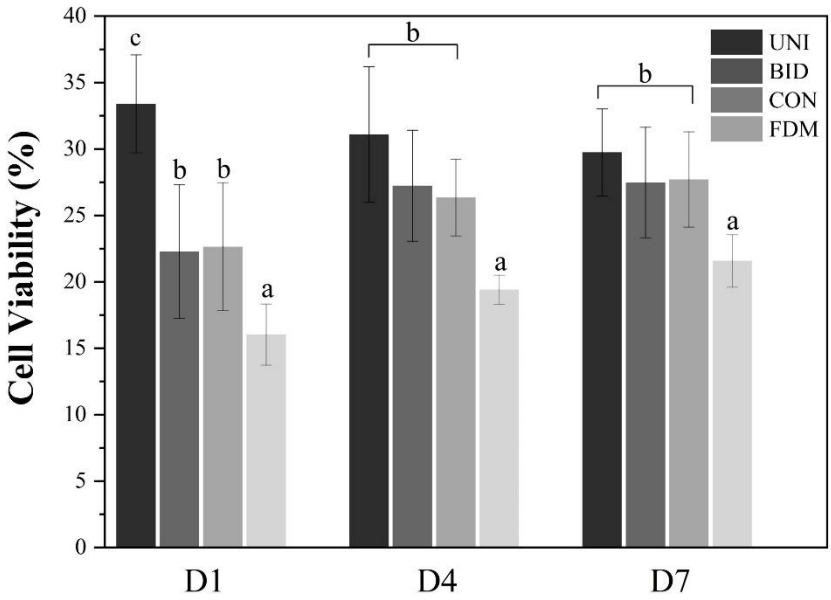

<Fig 12> WST-1 reagent test results for UNI, BID, CON, and FDM groups on D1, D4, and D7. Differences in lowercase alphabetical letters indicate significant differences between the groups ($n = 6$, $p < 0.05$).

연세대학교
YONSEI UNIVERSITY

3.6.2. Qualitative analysis

From a qualitative standpoint, LIVE/DEAD staining images showed that the FDM group had the most dead cells, which aligned with the WST-1 test results (Fig. 13). However, compared with the FDM group, the images of the 3D pen group appeared to be incomplete, with only ridge-like parts. In the CON group, cells appeared in a doughnut shape (white box), consistent with the concentric printing direction. In the combined UNI and BID groups, living cells were likely to be found at high elevations.

연세대학교
YONSEI UNIVERSITY

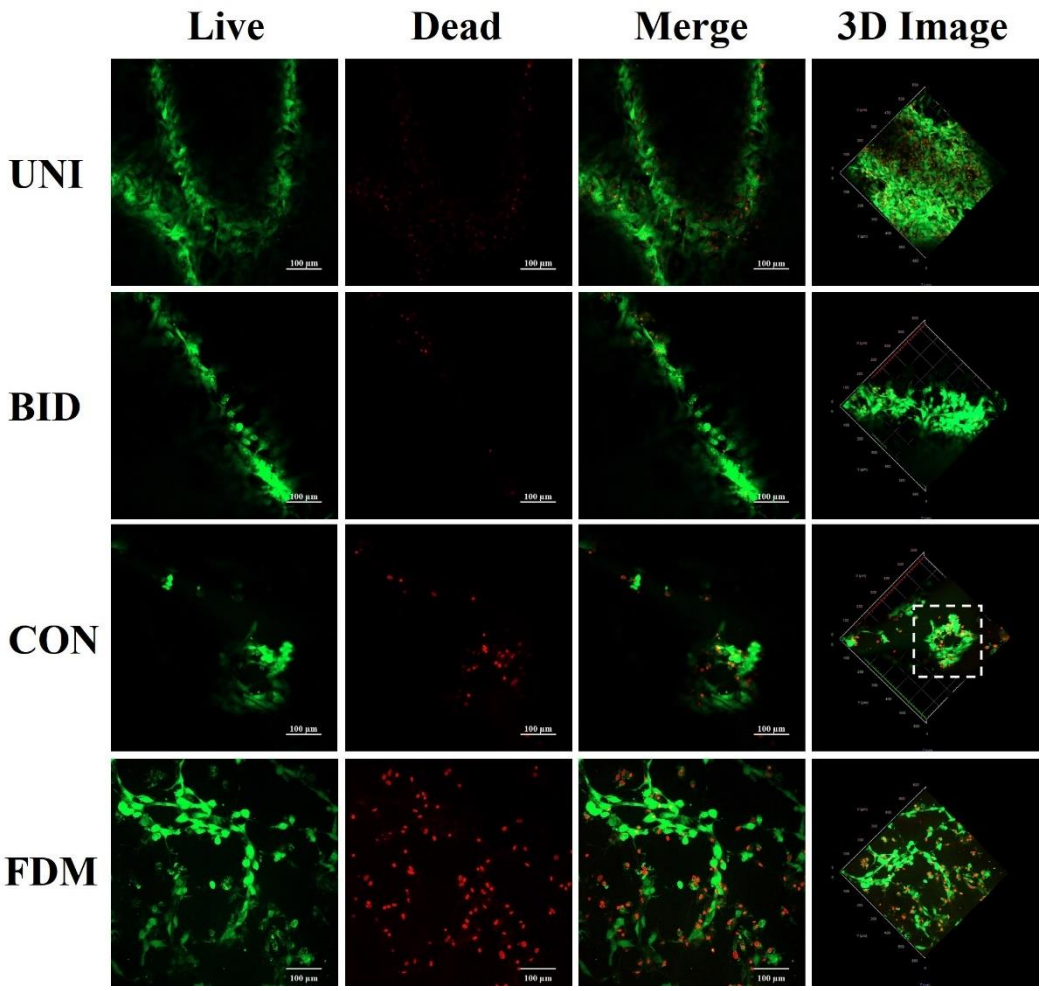

<Fig 13> 2D and 3D LIVE/DEAD staining images of groups UNI, BID, CON, and FDM. Green represents live cells and red represents dead cells. The cells marked within the white box grew along the concentric printing direction. The scale bar at the bottom right corner of the image represents 100 micrometers.

연세대학교
YONSEI UNIVERSITY

3.7. Cell attachment results

In the SEM images of the cell attachment experiments, the patterns of the 3D pen-printed scaffolds could be distinctly observed (Fig. 14). Yellow dotted lines indicate the area where two printed filaments were in contact, where the terrain was the lowest. Over the course of three days, all groups of cells grew with an increasing number of cells. By the third day, FDM group cells began to aggregate at the edge of the scaffold, while no trace was found on the opposite side. For the 3D pen groups, especially in the CON group, cells clung to two adjacent filaments and grew across them.

Rhodamine–phalloidin staining images further revealed the biocompatibility and cell attachment ability characteristics of PCL scaffolds (Fig. 15). In both the 3D pen group and FDM group, pseudopods representing cell motility and exploration were visible, particularly when images were magnified 20 times. From the image of the CON group magnified by 20 times, the pseudopodia of cells can be clearly seen (white box).

연세대학교
YONSEI UNIVERSITY

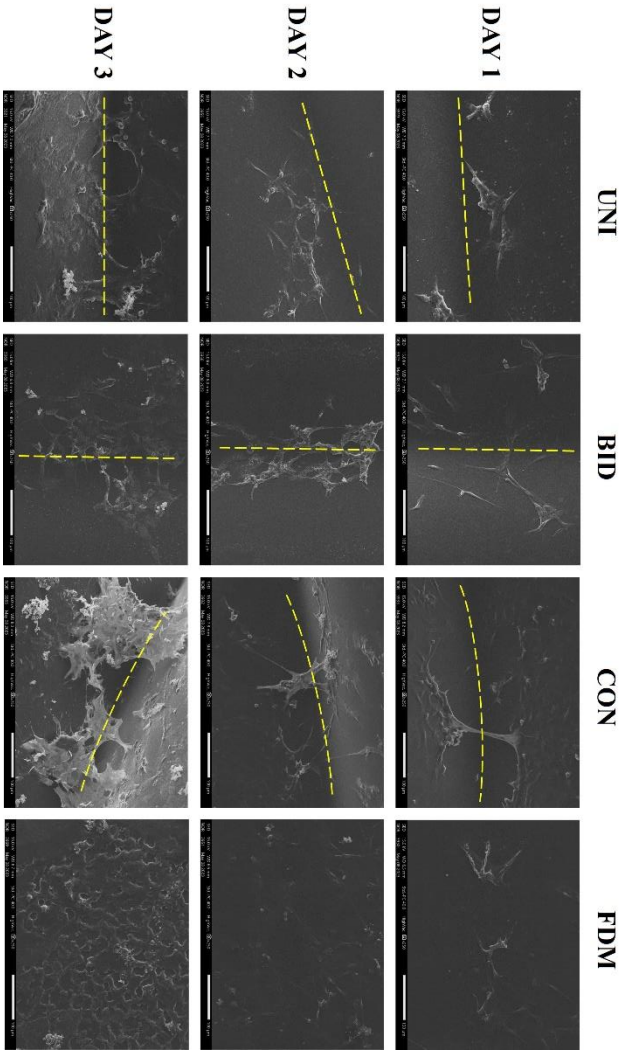

<Fig 14> SEM images of MC3T3-E1 attachment in groups UNI, BID, CON, and FDM within three days. The yellow dotted line indicates the direction of 3D pen printing and the patterns of the scaffolds. The scale bar at the bottom right corner of the image represents 100 micrometers.

연세대학교
YONSEI UNIVERSITY

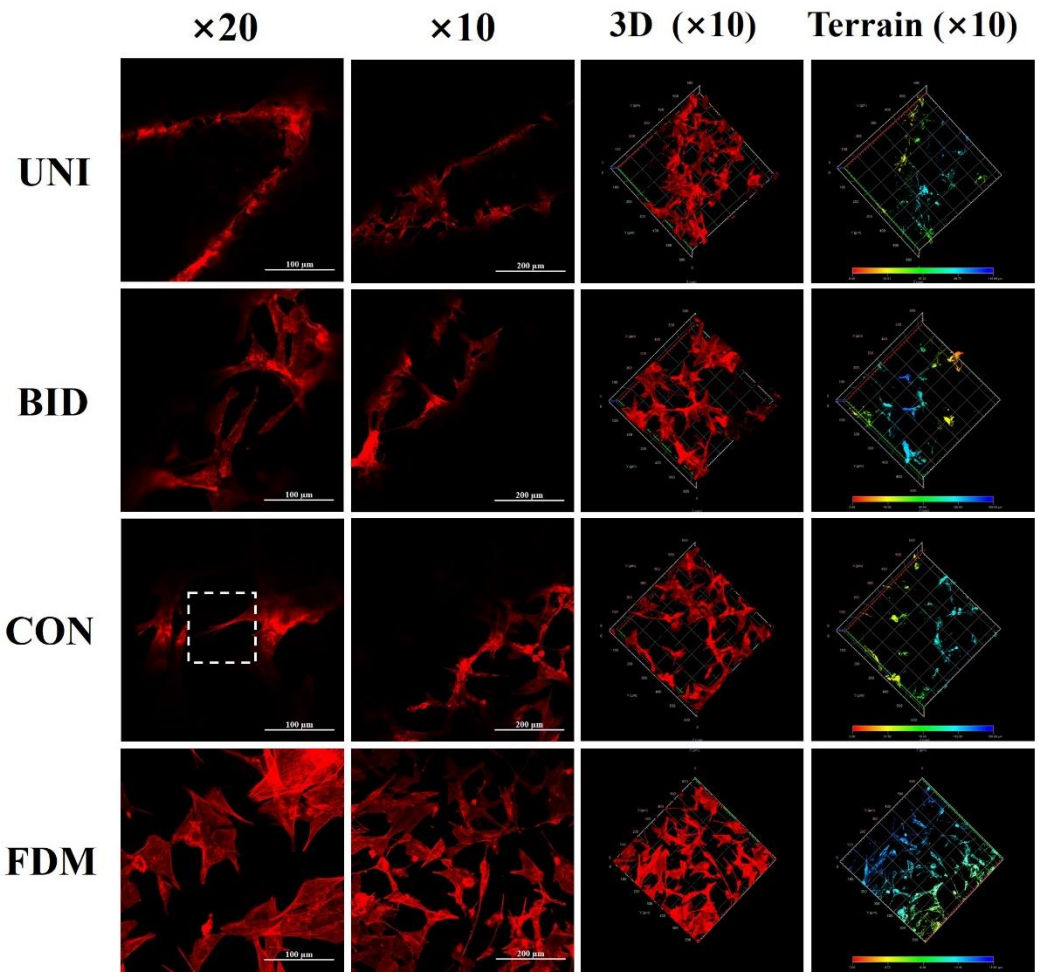

<Fig 15> ×10, ×20, 3D and terrain of ×10 Rhodamine-phalloidin staining images of groups UNI, BID, CON, and FDM. The white box marks the cell pseudopods. In the terrain maps, the colors represent different elevations: red indicates a higher elevation, while blue indicates a lower elevation. The scale bars at the bottom right corner of the image represent 100 and 200 micrometers respectively.

연세대학교
YONSEI UNIVERSITY

3.8. Simulated *in vitro* test results

In the test, the innovative application of industrial-grade modeling software to the fields of dentistry and bone regeneration was proposed because of its open and efficient system (Fig. 5c). As shown in Table 2, the dimensional deviation of the traditional digital design (6.7 %) was slightly higher than that of the 3D pen groups, taking much more time than the latter.

Table 2. Results of simulated *in vitro* tests. The durations were rounded to integer values.

	Time Spent (min)	**Dimensional Deviation (%)**
UNI 0°	4	5.0
UNI 90°	4	5.6
UNI 45°	4	5.5
BID 0°/90°	4	5.2
BID -45°/45°	4	5.5
CON	4	4.9
Workflow (FDM)	29	6.7

연세대학교
YONSEI UNIVERSITY

4. DISCUSSION

4.1. Mechanical characterization

The filaments produced by the FDM 3D printer were fine; despite setting the fill density to 100 %, tiny pores were present on the sides of the specimens not in contact with the platform (Fig. 7a) (Gordeev et al., 2018). Fine filaments and these pores contributed to the poor elastic moduli of the specimens printed by the FDM 3D printer (Gorecka et al., 2020). The above tensile test results indicated that for PCL samples, the bonding strength between each filament was considerably lower than the tensile strength of PCL itself. Therefore, the optimal resistance to stretching of the scaffold could be achieved by printing in a direction parallel to the applied force, providing a reference and theoretical basis for the future clinical applications of 3D pens.

The observed fluctuations of cures in the flexural test were a consequence of the layered structure of the sample, and the damage propagated from the bottom layer upwards, layer by layer, with the application of force over time, which is depicted in the image. According to the size requirements, the flexural specimen made by the 3D pen had four layers; thus, four obvious fluctuations could be observed in groups UNI 45° and UNI -45°/45°. Conversely, the curves of the UNI 0° group suggested that the scaffolds printed in the 0° direction had stable internal structures. However, Fig. 8b reveals that groups UNI 0°, UNI 45° and UNI -45°/45° all had good flexural strength, indicating that there was no direct correlation between the structural stability and maximum compressive strength of the scaffold.

The decrease in bond strength could be attributed to the shrinkage of PCL as the temperature decreased (Dash and Konkimalla, 2012). It could be assumed that the printing direction of the PCL scaffold did not significantly affect the shear bond performance with bone. The lack of bond test results in the FDM group was attributed to the fact that the 3D-printed scaffolds could not be directly used for bone repair, which has fixation and safety challenges (Table 1). In metal materials, bone plate holes are typically designed to address fixation issues, and 3D-printed polymer scaffolds require a suitable approach, while the 3D pen scaffolds do not encounter this problem (Liu et al., 2004; Tilton et al., 2020). PCL in the molten state could temporarily stably adhere to the bone, although the bond strength could decrease over time, as mentioned previously. Regarding safety concerns, the 3D pen technique eliminated the need for additional disinfection and sterilization during transportation, unlike traditional or 3D-printed scaffolds. The method simply required storage in a sterile environment with biofilaments, reducing labour and time costs.

연세대학교
YONSEI UNIVERSITY

4.2. Biological characterization

Although the cell viability of 3D pen groups was greater, it was still not optimal. Typically, Polycaprolactone had to be matched with other materials to play a highly effective role in the field of guided tissue regeneration and guided bone regeneration (GTR/GBR). Promising materials to consider for this purpose include magnesium (Mg) (Wang et al., 2022; Zhao et al., 2022), β-tricalcium (β-TCP) (Beatrice et al., 2020a; Ngo et al., 2023; Park et al., 2018), and hydroxyapatite (HA) (Park et al., 2011; Roohani-Esfahani et al., 2010), etc. Filament extruders could be utilized to fabricate customized composite filaments by adding these granular materials (Beatrice et al., 2020b; de Araujo et al., 2020). Novel composite filament designs and fabrication will be considered in subsequent research (Fig. 16).

In LIVE/DEAD staining images, the 3D pen groups appeared to be incomplete, with only ridge-like parts. This phenomenon occurred because the filament diameter extruded by the 3D pen was much thicker than that extruded by the FDM 3D printer, resulting in the surfaces of the 3D pen-printed scaffolds resembling an undulating hillside (Fig. 7b). CLSM photographs were optimally focused on a single horizontal plane, causing any part above or below this defined plane to be out of focus, as was the case with the 3D pen group images. Fortunately, 3D images were taken to compensate for this limitation, allowing the merging of multiple layers. In the CON group, cells appeared in a doughnut shape (white box), consistent with the concentric printing direction, indicating that the cells grew regularly along the printed filaments (Guarino et al., 2008).

In the SEM images of the cell attachment experiments, cells clung to two adjacent filaments and grew across them in 3D pen groups, demonstrating the support of PCL for cell adhesion (Huang et al., 2020). For rhodamine-phalloidin staining, 3D images and terrain images were selected to address the same issue as the LIVE/DEAD figures. Colour differences in terrain images helped identify the height of the terrain, facilitating the determination of the 3D printing filament direction and scaffold patterns. Terrian images of the FDM group revealed that the scaffold printed by the FDM 3D printer was not absolutely horizontal, which could explain the phenomenon that the cells only aggregated on one side in SEM images.

연세대학교
YONSEI UNIVERSITY

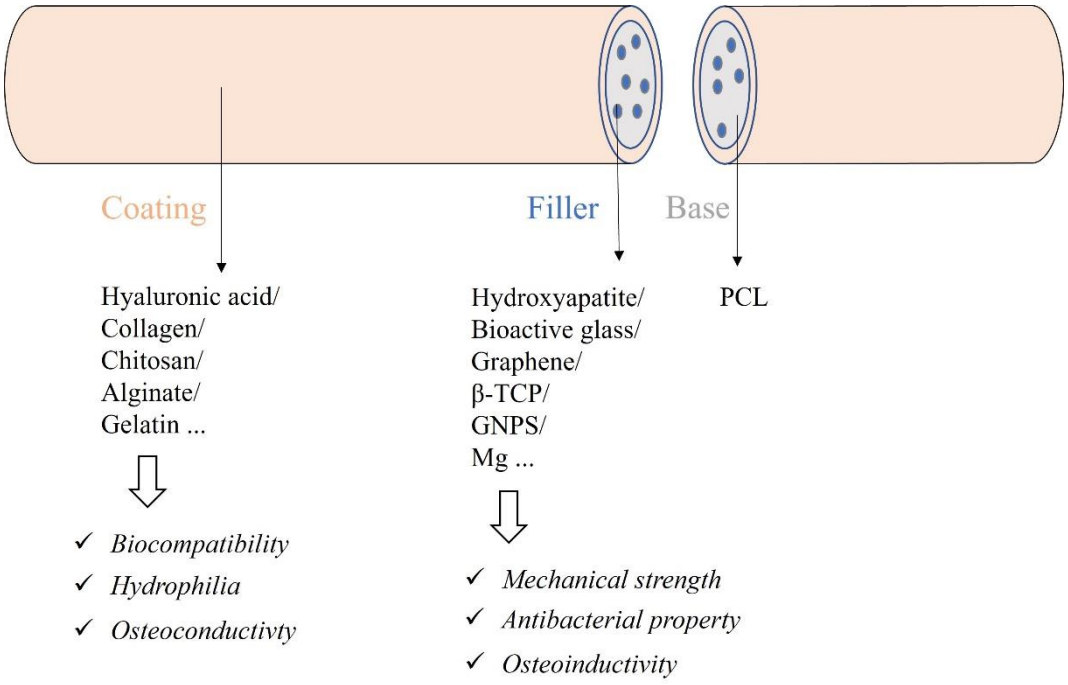

<Fig 16> Schematic diagram of new composite filaments.

연세대학교
YONSEI UNIVERSITY

4.3. Challenges and deficiencies

SEM images of the FDM group samples showed a filament orientation similar to that of the BID -45°/45° group. However, the BID -45°/45° group outperformed the FDM group in tensile, flexural, compression, and tear tests. This discrepancy may be attributed to the presence of pores in FDM-printed samples, which negatively impacted their mechanical properties. FDM printers offer various infill patterns such as grids, lines, triangles, cubic, octet, and zigzag (Fernandez-Vicente et al., 2016; Singh et al., 2022). Dezaki et al. demonstrated that infill patterns directly affect the surface quality and mechanical properties of 3D-printed products (Lalegani Dezaki et al., 2021). Fernandez-Vicente et al. found that, under equivalent density, the honeycomb pattern exhibited superior tensile strength compared to rectilinear and line patterns (Fernandez-Vicente et al., 2016). Furthermore, factors such as layer height, nozzle diameter, build orientation, and infill density also influence the mechanical properties of FDM-printed samples (Dave et al., 2019; Pandžić et al., 2021; Singh et al., 2022; Sriya Ambati and Ambatipudi, 2022). In this study, I exclusively used the grid infill pattern, meaning that our findings do not fully represent the capabilities of FDM printers. Additional research is needed to explore whether samples would perform better with different infill settings.

For the results of the simulated *in vitro* test, in addition to the errors introduced during the design step (Li et al., 2017), the shrinkage of the PCL scaffold during printing was identified as the main contributing factor (Fig. 5d). However, the scaffold of the 3D pen group offset some of the dimensional shrinkage due to its ability to bond with bone. Temperature also posed a challenge that 3D pen technology had to overcome. Typically, nerve heat damage occurs at temperatures above 43 ℃, while bone tissue could be damaged at temperatures higher than 55 ℃ (Diederich, 2005; Hillery and Shuaib, 1999). In experiments, it was observed that PCL could reach a flow state at 50 ℃, dissipating part of the heat in the air before contacting the bone tissue, and the temperature of real contact with bone was about 30 ℃. Furthermore, the *in vitro* experiments did not account for wet conditions. In actual surgical procedures, defect sites are typically saturated with blood, which can complicate the *in situ* printing of polymer scaffolds (Dimitriou et al., 2011; Henkel et al., 2013). Consequently, the shear bond strength and scaffold accuracy measured in this study may not fully represent real-world scenarios. Future research will incorporate wet conditions to better evaluate the *in situ* printing performance of the 3D pen. The improvement of the hydrophilic properties of PCL also requires further consideration.

연세대학교
YONSEI UNIVERSITY

4.4. Research potential and prospect

This research introduces a novel application of 3D pens in the realm of medical science, specifically within the domain of *in situ* bone repair. Leveraging the low melting point of PCL, I propose, for the first time, the concept of directly constructing scaffolds at bone defect sites using 3D pens. The versatility of 3D pens is anticipated to play a pivotal role in emergency (first aid) (Kim et al., 2017), military (traumatology) (Mishra et al., 2019), and various other fields. To cater to diverse needs, composite filaments based on PCL can be meticulously prepared in advance, sealed after disinfection, and conveniently carried by medical staff. These professionals can utilize 3D pens, along with different types of biofilaments, not only within operating theater but also in any clinical scenario. This innovation enables the swift construction of temporary scaffolds or biofilms, addressing requirements such as hemostasis, bone stress recovery, and more. Crucially, the 3D pen's ability to accomplish these tasks in a short timeframe without the constraints of instruments, software, or network dependencies sets it apart from traditional digital repair technologies. While there are currently limited studies on 3D pens, some articles have indicated that, akin to FDM 3D printers, 3D pens may emit ultrafine particles (UFPs) during operation, potentially posing a risk to human health, which needs further verification (Kim and Lee, 2022; Sigloch et al., 2020).

Furthermore, although the ability of FDM 3D printers to process some irregular model details could need improvement (Penumakala et al., 2020; Wickramasinghe et al., 2020), the influence of 3D printing technology on the present era could not be denied. 3D printing technology exhibited a high precision, as shown by the above experimental results (standard deviation), holding irreplaceable significance for industrial production (Ford and Despeisse, 2016; Ngo et al., 2018; Xiong et al., 2022). In the medical field, 3D printers could usually play a better role in some high-stress requirements or precision miniature scaffolds (Kang et al., 2016; Lee et al., 2019; Salmi, 2021). Additionally, despite the use of a cattle femur model to simulate the bone repair process in this study, *in vivo* experiments remain crucial. These experiments are planned for subsequent studies to evaluate PCL-based composite scaffolds using the 3D pen. Such experiments are anticipated to more intuitively showcase the capabilities of the 3D pen and demonstrate its characteristics of speed, convenience, and accuracy.

연세대학교
YONSEI UNIVERSITY

5. CONCLUSION

In this work, 3D pen was proposed as a novel strategy for *in situ* bone repair. The mechanical and biological properties of 3D pen-printed scaffolds in six patterns were evaluated. Furthermore, the process of creating a bone repair scaffold was simulated using an FDM 3D printer and a 3D pen to compare the time required and accuracy of the achieved scaffolds.

The results were as follows;

(1) Regarding mechanical properties, 3D pen-printed scaffolds with different patterns exhibited varying results in four tests, except for the shear bond test. The optimal strength of the scaffold could be achieved by printing in a direction parallel to the applied force.

(2) For biological properties, 3D pen-printed scaffolds with various patterns exhibited consistent cell viability over time and demonstrated excellent cell attachment capabilities overall. Moreover, the study revealed that cells grew along the printed filaments regularly, with additional living cells being found at high elevations.

(3) In simulated *in vitro* tests, the 3D pen outperformed traditional digital technology with an FDM 3D printer in terms of accuracy and speed.

Since the null hypothesis was rejected, these findings underscored the tremendous potential of the 3D pen in the field of immediate treatment, indicating that it could serve as a viable alternative to FDM 3D printers in specific applications.

연세대학교
YONSEI UNIVERSITY

References

Amini AR, Laurencin CT, Nukavarapu SP: Bone tissue engineering: Recent advances and challenges. Crit. Rev. Biomed. Eng. 40(5):363–408, 2012.

Arora JK, Bhati P: Fabrication and characterization of 3D printed PLA scaffolds. In: Proceedings of the 35th International Conference of the Polymer Processing Society (Pps-35). Melville NY, US: AIP Publishing, 2020.

Beatrice CAG, Shimomura KMB, Backes EH, Harb SV, Costa LC, Passador FR, et al.: Engineering printable composites of poly (ε-polycaprolactone) / β-tricalcium phosphate for biomedical applications. Polymer Composites 42(3):1198-1213, 2020a.

Bose S, Roy M, Bandyopadhyay A: Recent advances in bone tissue engineering scaffolds. Trends Biotechnol. 30(10):546–554, 2012.

Bose S, Vahabzadeh S, Bandyopadhyay A: Bone tissue engineering using 3D printing. Mater. Today 16(12):496–504, 2013.

Campbell PG, Weiss LE: Tissue engineering with the aid of inkjet printers. Expert Opin Biol Ther 7(8):1123-1127, 2007.

Chaudhry MS, Czekanski A: In-situ bioprinting of skin - A review. Bioprinting 31, 2023.

Dash TK, Konkimalla VB: Poly-ϵ-caprolactone based formulations for drug delivery and tissue engineering: A review. J. Control. Release 158(1):15–33, 2012.

de Araujo FP, Batista ITS, de Oliveira FC, de Almeida LR, Brito GDC, Barud HDS, et al.: Printing composite nanofilaments for use in a simple and low-cost 3D pen. J. Mater. Res. 35(9):1154–1162, 2020.

de Oliveira FM, de Melo EI, da Silva RAB: 3D Pen: A low-cost and portable tool for manufacture of 3D-printed sensors. Sensors and Actuators B: Chemical 321, 2020.

Diederich CJ: Thermal ablation and high-temperature thermal therapy: Overview of technology and clinical implementation. Int. J. Hyperth. 21(8):745–753, 2005.

Dimitriou R, Jones E, McGonagle D, Giannoudis PV: Bone regeneration: Current concepts and

연세대학교
YONSEI UNIVERSITY

future directions. BMC Med. 9:66, 2011.

Ford S, Despeisse M: Additive manufacturing and sustainability: An exploratory study of the advantages and challenges. J. Clean. Prod. 137:1573–1587, 2016.

Gordeev EG, Galushko AS, Ananikov VP: Improvement of quality of 3D printed objects by elimination of microscopic structural defects in fused deposition modeling. PLoS One 13(6):e0198370, 2018.

Gorecka Z, Idaszek J, Kolbuk D, Choinska E, Chlanda A, Swieszkowski W: The effect of diameter of fibre on formation of hydrogen bonds and mechanical properties of 3D-printed PCL. Mater. Sci. Eng. Mater. Biol. Appl. 114:111072, 2020.

Guarino V, Causa F, Taddei P, di Foggia M, Ciapetti G, Martini D, et al.: Polylactic acid fibre-reinforced polycaprolactone scaffolds for bone tissue engineering. Biomaterials 29(27):3662-3670, 2008.

Henkel J, Woodruff MA, Epari DR, Steck R, Glatt V, Dickinson IC, et al.: Bone regeneration based on tissue engineering conceptions - A 21st century perspective. Bone Res. 1(3):216–248, 2013.

Hillery MT, Shuaib I: Temperature effects in the drilling of human and bovine bone. J. Mater. Process. Technol. 92-93:302–308, 1999.

Hollister SJ: Porous scaffold design for tissue engineering. Nat. Mater. 4(7):518–524, 2005.

Huang B, Aslan E, Jiang Z, Daskalakis E, Jiao M, Aldalbahi A, et al.: Engineered dual-scale poly (ε-caprolactone) scaffolds using 3D printing and rotational electrospinning for bone tissue regeneration. Addit. Manuf. 36:101452, 2020.

Kaiser LR: The future of multihospital systems. Top. Health Care Financ. 18(4):32–45, 1992.

Kang HW, Lee SJ, Ko IK, Kengla C, Yoo JJ, Atala A: A 3D bioprinting system to produce human-scale tissue constructs with structural integrity. Nat Biotechnol 34(3):312-319, 2016.

Kim D, Lee K: Characteristics of ultrafine particles emitted from 3D-pens and effect of partition on children's exposure during 3D-pen operation. Indoor Air 32(1):e12978, 2022.

Kim YC, Jeong WS, Park TK, Choi JW, Koh KS, Oh TS: The accuracy of patient specific implant prebented with 3D-printed rapid prototype model for orbital wall reconstruction. J Craniomaxillofac Surg 45(6):928-936, 2017.

연세대학교
YONSEI UNIVERSITY

Langer R, Vacanti JP: TISSUE ENGINEERING. Science 260(5110):920-926, 1993.

Lee A, Hudson AR, Shiwarski DJ, Tashman JW, Hinton TJ, Yerneni S, et al.: 3D bioprinting of collagen to rebuild components of the human heart. Science 365(6452):482-487, 2019.

Li L, Yu F, Shi J, Shen S, Teng H, Yang J, et al.: In situ repair of bone and cartilage defects using 3D scanning and 3D printing. Sci. Rep. 7(1):9416, 2017.

Ligon SC, Liska R, Stampfl J, Gurr M, Mülhaupt R: Polymers for 3D printing and customized additive manufacturing. Chem. Rev. 117(15):10212–10290, 2017.

Liu X, Chu P, Ding C: Surface modification of titanium, titanium alloys, and related materials for biomedical applications. Mater. Sci. Eng. Rep. 47(3-4):49–121, 2004.

MacAdam A, Chaudry E, McTiernan CD, Cortes D, Suuronen EJ, Alarcon EI: Development of in situ bioprinting: A mini review. Front Bioeng Biotechnol 10:940896, 2022.

Mahmoudi Z, Sedighi M, Jafari A, Naghieh S, Stefanek E, Akbari M, et al.: In situ 3D bioprinting: A promising technique in advanced biofabrication strategies. Bioprinting 31, 2023.

Mishra A, Verma T, Vaish A, Vaish R, Vaishya R, Maini L: Virtual preoperative planning and 3D printing are valuable for the management of complex orthopaedic trauma. Chin J Traumatol 22(6):350-355, 2019.

Mishra PK, Senthil P, Adarsh S, Anoop MS: An investigation to study the combined effect of different infill pattern and infill density on the impact strength of 3D printed polylactic acid parts. Compos. Commun. 24:100605, 2021.

Ngo ST, Lee WF, Wu YF, Salamanca E, Aung LM, Chao YQ, et al.: Fabrication of Solvent-Free PCL/beta-TCP Composite Fiber for 3D Printing: Physiochemical and Biological Investigation. Polymers (Basel) 15(6), 2023.

Ngo TD, Kashani A, Imbalzano G, Nguyen KTQ, Hui D: Additive manufacturing (3D printing): A review of materials, methods, applications and challenges. Compos. Eng. 143:172–196, 2018.

Park SA, Lee HJ, Kim KS, Lee SJ, Lee JT, Kim SY, et al.: In vivo evaluation of 3D-printed polycaprolactone scaffold implantation combined with beta-TCP powder for alveolar bone augmentation in a beagle defect model. Materials (Basel) 11(2):238, 2018.

Park SA, Lee SH, Kim WD: Fabrication of porous polycaprolactone/hydroxyapatite (PCL/HA) blend scaffolds using a 3D plotting system for bone tissue engineering. Bioprocess Biosyst Eng

연세대학교
YONSEI UNIVERSITY

34(4):505-513, 2011.

Penumakala PK, Santo J, Thomas A: A critical review on the fused deposition modeling of thermoplastic polymer composites. Compos. Eng. 201:108336, 2020.

Pierantozzi D, Scalzone A, Jindal S, Stīpniece L, Šalma-Ancāne K, Dalgarno K, et al.: 3D printed Sr-containing composite scaffolds: Effect of structural design and material formulation towards new strategies for bone tissue engineering. Compos. Sci. Technol. 191:108069, 2020.

Puppi D, Chiellini F, Piras AM, Chiellini E: Polymeric materials for bone and cartilage repair. Prog. Polym. Sci. 35(4):403–440, 2010.

Rekow ED: Digital dentistry: The new state of the art-Is it disruptive or destructive? Dent. Mater. 36(1):9–24, 2020.

Roohani-Esfahani SI, Nouri-Khorasani S, Lu Z, Appleyard R, Zreiqat H: The influence hydroxyapatite nanoparticle shape and size on the properties of biphasic calcium phosphate scaffolds coated with hydroxyapatite-PCL composites. Biomaterials 31(21):5498-5509, 2010.

Roseti L, Parisi V, Petretta M, Cavallo C, Desando G, Bartolotti I, et al.: Scaffolds for bone tissue engineering: State of the art and new perspectives. Mater. Sci. Eng. Mater. Biol. Appl. 78:1246–1262, 2017.

Salerno A, Palladino A, Pizzoleo C, Attanasio C, Netti PA: Computer-aided patterning of PCL microspheres to build modular scaffolds featuring improved strength and neovascularized tissue integration. Biofabrication 14(2):101, 2022.

Salmi M: Additive manufacturing processes in medical applications. Materials (Basel) 14(1):191, 2021.

Shahverdi M, Seifi S, Akbari A, Mohammadi K, Shamloo A, Movahhedy MR: Melt electrowriting of PLA, PCL, and composite PLA/PCL scaffolds for tissue engineering application. Sci. Rep. 12(1):19935, 2022.

Shen J, Wang W, Zhai X, Chen B, Qiao W, Li W, et al.: 3D-printed nanocomposite scaffolds with tunable magnesium ionic microenvironment induce in situ bone tissue regeneration. Appl. Mater. Today 16:493–507, 2019.

Sigloch H, Bierkandt FS, Singh AV, Gadicherla AK, Laux P, Luch A: 3D Printing - Evaluating Particle Emissions of a 3D Printing Pen. J Vis Exp (164), 2020.

연세대학교
YONSEI UNIVERSITY

Singh J, Goyal KK, Kumar R, Gupta V: Influence of process parameters on mechanical strength, build time, and material consumption of 3D printed polylactic acid parts. Polymer Composites 43(9):5908-5928, 2022.

Singh S, Choudhury D, Yu F, Mironov V, Naing MW: In situ bioprinting - Bioprinting from benchside to bedside? Acta Biomater 101:14-25, 2020.

Sinha VR, Bansal K, Kaushik R, Kumria R, Trehan A: Poly-epsilon-caprolactone microspheres and nanospheres: An overview. Int. J. Pharm. 278(1):1–23, 2004.

Sriya Ambati S, Ambatipudi R: Effect of infill density and infill pattern on the mechanical properties of 3D printed PLA parts. Materials Today: Proceedings 64:804-807, 2022.

Staffa G, Barbanera A, Faiola A, Fricia M, Limoni P, Mottaran R, et al.: Custom made bioceramic implants in complex and large cranial reconstruction: A two-year follow-up. J. Cranio-Maxillofac. Surg. 40(3):e65–e70, 2012.

Stevens MM: Biomaterials for bone tissue engineering. Mater. Today 11(5):18–25, 2008.

Tilton M, Lewis GS, Bok WH, Armstrong A, Hast MW, Manogharan G: Additive manufacturing of fracture fixation implants: Design, material characterization, biomechanical modeling and experimentation. Addit. Manuf. 33:101137, 2020.

Wang F, Xia D, Wang S, Gu R, Yang F, Zhao X, et al.: Photocrosslinkable Col/PCL/Mg composite membrane providing spatiotemporal maintenance and positive osteogenetic effects during guided bone regeneration. Bioact. Mater. 13:53–63, 2022.

Wickramasinghe S, Do T, Tran P: FDM-based 3D printing of polymer and associated composite: A review on mechanical properties, defects and treatments. Polymers (Basel) 12(7):191, 2020.

Woodruff MA, Hutmacher DW: The return of a forgotten polymer—polycaprolactone in the 21st century. Prog. Polym. Sci. 35(10):1217–1256, 2010.

Xie M, Shi Y, Zhang C, Ge M, Zhang J, Chen Z, et al.: In situ 3D bioprinting with bioconcrete bioink. Nat Commun 13(1):3597, 2022.

Xiong Y, Tang Y, Zhou Q, Ma Y, Rosen DW: Intelligent additive manufacturing and design: State of the art and future perspectives. Addit. Manuf. 59:103139, 2022.

Yang Y, Wang G, Liang H, Gao C, Peng S, Shen L, et al.: Additive manufacturing of bone scaffolds. Int J Bioprint 5(1):148, 2019.

연세대학교
YONSEI UNIVERSITY

Zaldivar RJ, Witkin DB, McLouth T, Patel DN, Schmitt K, Nokes JP: Influence of processing and orientation print effects on the mechanical and thermal behavior of 3D-Printed ULTEM (R) 9085 Material. Addit. Manuf. 13:71–80, 2017.

Zhang S, Li X, Qi Y, Ma X, Qiao S, Cai H, et al.: Comparison of autogenous tooth materials and other bone grafts. Tissue Eng. Regen. Med. 18(3):327–341, 2021.

Zhao R, Yang R, Cooper PR, Khurshid Z, Shavandi A, Ratnayake J: Bone grafts and substitutes in dentistry: A review of current trends and developments. Molecules 26(10):3007, 2021.

Zhao X, Wang S, Wang F, Zhu Y, Gu R, Yang F, et al.: 3D-printed Mg-1Ca/polycaprolactone composite scaffolds with promoted bone regeneration. Journal of Magnesium and Alloys, 2022.

Zhou J, Huang H, Wang L-J, Tamaddon M, Liu C-Z, Liu Z-Y, et al.: Stable mechanical fixation in a bionic osteochondral scaffold considering bone growth. Rare Metals 41(8):2711-2718, 2022.

연세대학교
YONSEI UNIVERSITY

Abstract in Korean

3D 펜으로 제작된 다양한 패턴의 폴리카프로락톤 스캐폴드의 기계적 및 생물학적 특성 평가: 새로운 *in situ* 골 재생 전략

골조직공학(BTE) 분야에 대한 관심과 발전은 1980년대 중반 이후로 연구논문의 발표가 급격히 증가하면서 크게 성장하였다. BTE의 세 가지 요소 중 하나인 스캐폴드는 골 결손 부위의 안정성을 장기간 유지하고 골모세포와 혈관의 성장에 유리한 환경을 제공하는 능력으로 인해 널리 연구되고 선호되었다.

3D 프린팅 기술을 활용한 다단계 디지털 복원 과정이 높은 비용과 긴 주기를 동반하는 문제를 해결하기 위해, 현장에서(*in situ*) 골 재생을 위한 혁신적인 전략으로 3D 펜이 제안되었다. *In situ*는 살아있는 생물체 내 또는 자연 생물 환경에서 발생하는 과정을 의미한다. Polycaprolactone(PCL)의 낮은 융점 특성을 활용하여 처음으로 3D 펜을 이용해 골 결손 부위에서 직접 스캐폴드를 제작하는 새로운 개념이 도입하였다.

본 체외 연구(*in vitro*)는, 3D 펜으로 프린트된 PCL 지지체의 기계적 및 생물학적 특성을 면밀히 평가했다. 평가한 텍스처는 일방향(UNI 0°, 45°, 90°), 양방향(BID -45°/45°, 0°/90°), 그리고 동심원형(CON)의 총 6가지였다. 골 수복 지지체 제작 과정은 FDM(융합 적층 모델링) 3D 프린터와 3D 펜을 사용해 소의 골 결손 모델을 제작하여 시간 효율성과 정확성을 비교하는 방식으로 시뮬레이션하였다. 기계적 실험 결과, 3D 펜으로 프린트된 지지체는 전단 결합 실험 결과를 제외한 4개의 실험에서 텍스처에 따라 다양한 결과를 보였다. 지지체의 최적 강도는 인가된 힘과 평행하게 프린팅할 때인 것으로 나타났다. 생물학적 특성에 있어, 이러한 지지체는 시간이 지남에 따라 일관된 세포 생존율을 나타냈고, 전반적으로 우수한 세포 부착 능력을 보여주었다. 또한, 세포는 프린트된 필라멘트를 따라 규칙적으로 성장했으며, 더 높은 위치에서는 추가적인 생존 세포들이 관찰되었다. 추가적으로, 3D 펜 방법은 정확도와 속도 면에서 FDM 3D 프린터를 사용하는 전통적인 디지털 기술보다 우수한 성과를 보였다.

이러한 결과는 저비용, 고속, 편리함으로 특징지어지는 3D 펜이 의료 과학, 특히 골 조직 공학 분야에서 엄청난 잠재력을 가지고 있음을 보여주었다.

핵심되는 말 : 조직 공학, 스캐폴드, 폴리카프로락톤, 3D 펜, *in situ* 프린팅